A Blind Maximum-SINR Synchronization Technique for OFDM Systems

Wen-Long Chin and Sau-Gee Chen
Department of Electronics Engineering and Institute of Electronics
National Chiao Tung University
1001 Ta Hsueh Rd, Hsinchu, 30050, Taiwan, ROC
e-mail: johnsonchin@pchome.com.tw

***Abstract*—This work presents a blind synchronizer for orthogonal frequency-division multiplexing (OFDM) systems based on signal-to-interference-and-noise-ratio (SINR) maximization. Due to the incurred losses from inter-symbol interference (ISI) and inter-carrier interference (ICI) introduced by synchronization errors, the SINR of the received data drops drastically. By taking advantage of this characteristic, both the symbol time and carrier frequency offsets are intuitively estimated by maximizing the SINR metric. For the SINR metric, we propose a blind SINR estimation, which does not need prior knowledge of the channel profiles and transmitted data. As such, the proposed maximum-SINR (MSINR) synchronization algorithm is non-data-aided (NDA) so that the transmission efficiency can be improved. Moreover, to reduce the computational complexity, the early-late gate (ELG) technique is proposed for the implementation of the synchronizer. Simulation results exhibit better performance for the MSINR algorithm than conventional techniques in multipath fading channels.**

I. Introduction

Orthogonal frequency-division multiplexing (OFDM) is a promising technology for broadband transmission due to its high spectrum efficiency, and its robustness to the effects of multipath fading channels. However, it is sensitive to synchronization errors. First, uncertain OFDM symbol arrival time introduces a symbol time offset (STO). Second, the mismatch of the oscillators in carrier frequencies (CF) between the transmitter and the receiver produces a carrier frequency offset (CFO).

The symbol time (ST) estimation is usually the first step in an entire OFDM synchronization process, because it provides an estimated symbol boundary for the remaining synchronization steps. When the ST is not located in the inter-symbol-interference-free region, the inter-symbol-interference (ISI) will be inevitable. The CFO introduces additional inter-carrier interference (ICI).

In [1], the STO and CFO are jointly estimated by a delayed-correlation algorithm. It is a maximum-likelihood (ML) estimation and only good for the additive white Gaussian noise (AWGN) channel. Some techniques [2]-[3] have good ST performances. However, extra time-domain training symbols are needed. In [3] and [4], the channel frequency response (CFR) must be estimated first. The inverse fast Fourier transform (IFFT) is then applied to obtain the channel impulse response (CIR), which is then used to adjust the symbol boundary. Some works locate the symbol boundary at the sampling point that has the minimum-interference [5]-[6].

The proposed scheme is to effectively reduce the synchronization errors, including the STO and the CFO, so that the signal-to-interference-and-noise-ratio (SINR) is maximized. In other words, not only the interference power is considered but also the signal power. A blind SINR estimation is proposed for the maximum-SINR (MSINR) synchronization algorithm. As such, the proposed MSINR algorithm is non-data-aided (NDA) such that the bandwidth efficiency can be improved. In addition, to reduce the computational complexity, the early-late gate (ELG) technique is also proposed for the implementation of the new MSINR algorithm.

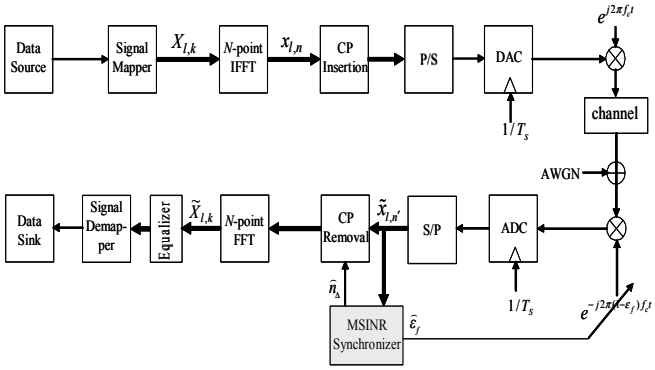

Fig. 1. A simplified OFDM system model. The MSINR synchronizer operates in frequency domain by utilizing the FFT operations. Detailed block diagram of the synchronizer can be found in Fig. 3.

The rest of this paper is organized as follows. The OFDM system and signal models are introduced in Section II. The blind SINR estimation, MSINR synchronization algorithm, and the ELG technique are then detailed and analyzed in Section III. The performance is analyzed in Section IV. Simulation results are provided in Section V. Finally, we conclude our work in Section VI.

II. OFDM System and Signal Models

In the following discussion, all the quantities indexed with l belong to the l-th symbol. A simplified OFDM system model is shown in Fig. 1. In this figure, $X_{l,k}$ / $\tilde{X}_{l,k}$ is the transmitted/received frequency-domain data at the k-th subcarrier; $x_{l,n}$ is the transmitted time-domain data after the IFFT; $\tilde{x}_{l,n'}$ is the received time-domain data, where $-N_G \le n' < N$, N is the number of subcarriers, and N_G is the cyclic prefix (CP) length; $1/T_S$ is the sampling frequency; ε_f is the CFO divided by f_c, where f_c is the carrier frequency; $\hat{n}_\Delta$ is the estimated STO; and $\hat{\varepsilon}_f$ is the estimated CFO divided by f_c. On the transmitter side, N complex data symbols are modulated onto N subcarriers by

978-1-4244-2324-8/08/$25.00 © 2008 IEEE.

This full text paper was peer reviewed at the direction of IEEE Communications Society subject matter experts for publication in the IEEE "GLOBECOM" 2008 proceedings.

using the IFFT. The last N_G IFFT output samples are copied to form the CP that is inserted at the beginning of each OFDM symbol. By inserting the CP, a guard interval is created so that ISI can be avoided and the orthogonality among subcarriers can be sustained. The receiver uses the fast Fourier transform (FFT) to demodulate received data.

The estimated ST generally falls into one of the three regions of an OFDM symbol: the Bad-ST1 region, the Good-ST region (also known as the ISI-free region), and the Bad-ST2 region in which the STO n_Δ, is confined within the ranges of $-N_G \le n_\Delta \le -N_G + \tau_d - 1$, $-N_G + \tau_d \le n_\Delta \le 0$, and $1 \le n_\Delta \le N-1$, respectively, where τ_d is the maximum delay spread of the channel. Detailed analysis of the received frequency-domain data (at the *k*-th subcarrier) in these three regions can be found in [7], and rewritten below (for only the Bad-ST2 region)

$$\tilde{X}_{l,k} = \tilde{X}^d_{l,k} + \tilde{N}_k \tag{1}$$

where

$$\tilde{X}^d_{l,k} \triangleq \frac{N-n_\Delta}{N} H_k X_{l,k} W_N^{(-lN_s\varepsilon_f - kn_\Delta)} \tag{2}$$

is the desired data, H_k is the CFR at the *k*-th subcarrier, W_N is $e^{-j2\pi/N}$, and $N_S = N + N_G$ is the OFDM symbol length including the CP; and

$$\tilde{N}_k \triangleq \frac{1}{N}\sum_{m\neq k}\sum_{n'=0}^{N-1} W_N^{-n'(m-k+\varepsilon_f)} H_m X_{l,m} W_N^{(-lN_s\varepsilon_f - kn_\Delta)} + v_k - \tilde{X}^{ici}_{l,k} + \tilde{X}^{isi}_{l,k} \tag{3}$$

is the combined interference and the AWGN v_k, where

$$\tilde{X}^{ici}_{l,k} = \frac{1}{N}\sum_{m\neq k}\sum_{n'=N-n_\Delta}^{N-1} W_N^{-n'(m-k+\varepsilon_f)} H_m X_{l,m} W_N^{(-lN_s\varepsilon_f - kn_\Delta)} \tag{4}$$

is the ICI term, and

$$\tilde{X}^{isi}_{l,k} = \frac{1}{N}\sum_{m}\sum_{n'=N-n_\Delta}^{N-1} W_N^{-n'(m-k+\varepsilon_f)} H_m X_{l+1,m} W_N^{(-lN_s\varepsilon_f - k(n_\Delta+N_G))} \tag{5}$$

is the ISI term. It can be easily shown that the theoretical SINR is

$$\eta_{th}(n_\Delta, \varepsilon_f) = \sum_k \sigma^2_{\tilde{X}^d_{l,k}} \Big/ \sum_k \sigma^2_{\tilde{N}_k} \tag{6}$$

where

$$\sigma^2_{\tilde{X}^d_{l,k}} = \left(\frac{N-n_\Delta}{N}\right)^2 m_{|X|^2} \left|H_k\right|^2 \tag{7}$$

is the desired signal power,

$$\sigma^2_{\tilde{N}_k} = \frac{\sigma^2_X}{N^2}\left\{\sum_{m\neq k}\sum_{n_1=0}^{N-1}\sum_{n_2=0}^{N-1} W_N^{-(n_1-n_2)(m-k+\varepsilon_f)}\left|H_m\right|^2 + \sum_{n_1=N-n_\Delta}^{N-1}\sum_{n_2=N-n_\Delta}^{N-1} W_N^{-(n_1-n_2)\varepsilon_f}\left|H_k\right|^2 + 2\sum_{m\neq k}\sum_{n_1=N-n_\Delta}^{N-1}\sum_{n_2=N-n_\Delta}^{N-1} W_N^{-(n_1-n_2)(m-k+\varepsilon_f)}\left|H_m\right|^2 + \sigma^2_{v_k}\right\} \tag{8}$$

is the combined interference-and-the-AWGN power, σ^2_X is the transmitted data power, and $\sigma^2_{v_k}$ is the AWGN power.

III. Proposed MSINR Synchronization Technique

The signal power decreases while the interference power increases when the STO and/or the CFO increase [8]-[9], as also suggested in (7) and (8), respectively. Consequently, it is evident that the SINR is a good metric to indicate the synchronization offsets. In comparison, those minimum-interference synchronizers [5]-[6] considering only the interference power may have performance losses.

A. Blind SINR Estimation for MSINR Algorithm

Before introducing the MSINR synchronization technique, the SINR estimation for (6) is investigated first.

1) SINR Estimation Based on Coherence Function: The coherence function [10]-[11] is often used to determine the degree to which one observed signal is related to another observed signal. If we have uncorrelated noise and the coherent signal, the amount of the powers due to noise and coherent signal can be determined. The concept of coherence function can be applied to the OFDM systems, so that the SINR, at the *k*-th subcarrier of the *l*-th symbol, can be written as

$$\hat{\eta}_{l,k}(n_\Delta, \varepsilon_f) = \frac{\left|\hat{\gamma}_{l,k}\right|^2}{1-\left|\hat{\gamma}_{l,k}\right|^2} \tag{9}$$

where

$$\left|\hat{\gamma}_{l,k}\right|^2 \triangleq \frac{\left|E\left[\tilde{X}_{l,k}\tilde{X}^*_{l+1,k}\right]\right|^2}{E\left[\left|\tilde{X}_{l,k}\right|^2\right]E\left[\left|\tilde{X}_{l+1,k}\right|^2\right]},\ k\in P,\ 0\le\left|\hat{\gamma}_{l,k}\right|^2\le 1 \tag{10}$$

is the magnitude-squared coherence (MSC) at the *k*-th subcarrier of the *l*-th symbol, and *P* is the pilot set. The MSC is the cross-power spectrum of two consecutive symbols normalized by their auto-power spectra, which can be viewed as the correlation between like frequency components of the received frequency-domain data.

Originally, the MSC in [10] was realized by the commonly used technique of time sample average, which is based on the assumption of signal ergodicity. Besides, it is only applicable for data-aided (DA) systems. In OFDM systems, since there is only one data sample at each subcarrier within an OFDM symbol, and the channels are possibly time-selective fading, it is inadequate to realize the cross-correlation in (10) by averaging over data segments (or symbols). Therefore, to blindly

This full text paper was peer reviewed at the direction of IEEE Communications Society subject matter experts for publication in the IEEE "GLOBECOM" 2008 proceedings.

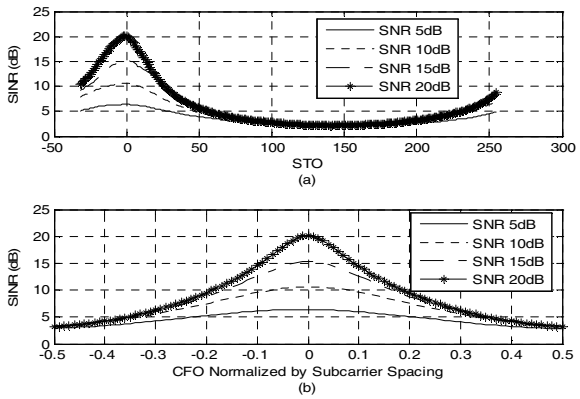

Fig. 2. The estimated SINR profiles against the STO and CFO in a multipath fading channel are shown in (a) and (b), respectively. $N = 256$. $L = 50$ symbols.

estimate the MSC without known data (or pilots) and derive the SINR profile in reasonable amounts of symbols, we propose to average the MSC over all N subcarriers within an OFDM symbol as follows

$$\overline{|\hat{\gamma}_l|}^2 = \frac{\left(\frac{1}{N}\sum_k \left|\tilde{X}_{l,k}\tilde{X}^*_{l+1,k}\right|\right)^2}{\left(\frac{1}{N}\sum_k \left|\tilde{X}_{l,k}\right|^2\right)\left(\frac{1}{N}\sum_k \left|\tilde{X}_{l+1,k}\right|^2\right)} \tag{11}$$

where the bar on top of $|\hat{\gamma}_l|$ denotes the sample average over N subcarriers. Finally, the SINR can be obtained by (9) as

$$\hat{\eta}_l(n_\Delta, \varepsilon_f) = \frac{\overline{|\hat{\gamma}_l|}^2}{1 - \overline{|\hat{\gamma}_l|}^2}. \tag{12}$$

Note that the SINR estimation (12) can be averaged over symbols to improve the accuracy.

2) Estimated SINR Profiles: We assume an OFDM system with the following specifications: $N = 256$, $N_G = 32$, $f_c = 2.4$ GHz, $T_s = 115.2\ \mu s$, and the signal bandwidth is 2.5 MHz. The SINR estimates (12) against the STO and CFO (normalized by the subcarrier spacing) in a multipath fading channel are demonstrated in Figs. 2(a) and 2(b), respectively. The channel is assumed to have N_G paths. The channel taps are randomly generated by independent zero-mean, complex Gaussian variables. As can be seen, the SINR estimates in Figs. 2(a) and 2(b) have the prominent peak values in the Good-ST region (at the 0th sample) and at CFO = 0, respectively. This figure also shows that how drastically the ISI/ICI is affected by the STO/CFO.

B. MSINR Synchronization Algorithm

1) MSINR Global Search Algorithm (MSINR-GSA): As observed and concluded above, the SINR drops drastically due to incurred interferences from the ICI and ISI. In addition, with (6)-(8), it can be shown that the SINR is a unimodal function of the STO and CFO, and has the maximum value at the ideal synchronization point. (Due to space limitation, this figure is not shown here). Hence, one can estimate the STO and CFO by intuitively maximizing the SINR estimation (12) as

$$(\hat{n}_{\Delta,GSA}(l), \hat{\varepsilon}_{f,GSA}(l)) = \arg\max_{n_\Delta, \varepsilon_f} \left\{\hat{\eta}_l(n_\Delta, \varepsilon_f)\right\} \tag{13}$$

where $\hat{n}_{\Delta,GSA}(l)$ and $\hat{\varepsilon}_{f,GSA}(l)$ are the l-th symbol's STO and CFO (divided by f_c) estimates of the two-dimensional MSINR-GSA, respectively. This is a complicated two-dimensional search problem. Since the SINR profile is a unimodal function of the STO and CFO, we separate it into two one-dimensional processes, i.e., the STO search and the CFO search, as described by the following equation

$$\begin{cases} \hat{n}'_{\Delta,GSA}(l) = \arg\max_{n_\Delta} \left\{\hat{\eta}_l(n_\Delta, \hat{\varepsilon}'_{f,GSA}(l-1))\right\} \\ \hat{\varepsilon}'_{f,GSA}(l) = \arg\max_{\varepsilon_f} \left\{\hat{\eta}_l(\hat{n}'_{\Delta,GSA}(l-1), \varepsilon_f)\right\} \end{cases}. \tag{14}$$

where $\hat{n}'_{\Delta,GSA}(l)$ and $\hat{\varepsilon}'_{f,GSA}(l)$ are the STO and CFO (divided by f_c) estimates of the one-dimensional MSINR-GSA.

2) MSINR-ELG ST (MSINR-ELG-ST) Recovery Loop: The computational complexity of (14) is still high, because the frequency-domain data and their SINRs have to be obtained over all possible synchronization points. To reduce the computational complexity, instead of searching the whole range of n_Δ, it is assumed that the signal is sampled early at $\hat{n}_{\Delta,ELG}(l) - \tau_\Delta$ and late at $\hat{n}_{\Delta,ELG}(l) + \tau_\Delta$, where $\hat{n}_{\Delta,ELG}(l)$ is the estimated STO of the MSINR-ELG-ST, and τ_Δ is the time shift relative to the estimated symbol boundary. The metrics (12) at these two symbol boundaries are subtracted and filtered to form an error signal $e_\Delta(l)$ [6]. The nonzero error signal is produced to fine-tune the symbol boundary and iteratively make the error signal become zero. The S-curve of the timing discriminator is given by

$$\begin{aligned} e_\Delta(l+1) = {} & \hat{\eta}_{l+1}(\hat{n}_{\Delta,ELG}(l) - \tau_\Delta, \hat{\varepsilon}_{f,ELG}(l)) \\ & - \hat{\eta}_{l+1}(\hat{n}_{\Delta,ELG}(l) + \tau_\Delta, \hat{\varepsilon}_{f,ELG}(l)) \end{aligned} \tag{15}$$

where $\hat{\varepsilon}_{f,ELG}(l)$ is the estimated CFO (divided by f_c) of the l-th symbol.

The MSINR ST synchronizer implemented by the ELG is shown in Fig. 3(a). An approximated linear model for the ELG timing recovery loop is shown in Fig. 4, where $F(z)$ is the loop filter, K_F is the loop filter gain, K_I is the timing detector's intrinsic gain, K_V is the voltage-controlled oscillator (VCO) gain, $N_\Delta(z)$ is the z-transform of n_Δ, $\hat{N}_\Delta(z)$ is the z-transform of $\hat{n}_{\Delta,ELG}(l)$, $E_\Delta(z)$ is the z-transform of $e_\Delta(l)$, and $E'_\Delta(z)$ is the z-transform of the filtered error signal $e'_\Delta(l)$. The ST is iteratively adjusted by the VCO as follows

$$\hat{n}_{\Delta,ELG}(l) = \hat{n}_{\Delta,ELG}(l-1) + K_V N_S T_S e'_\Delta(l). \tag{16}$$

The closed-loop system equation $L(z) \triangleq \hat{N}_\Delta(z) / N_\Delta(z)$ can be shown to be

$$L(z) = \frac{K_T z^{-1}(1 - az^{-1})}{1 + z^{-1}(K_T - 2) + z^{-2}(1 - K_T a)} \tag{17}$$

This full text paper was peer reviewed at the direction of IEEE Communications Society subject matter experts for publication in the IEEE "GLOBECOM" 2008 proceedings.

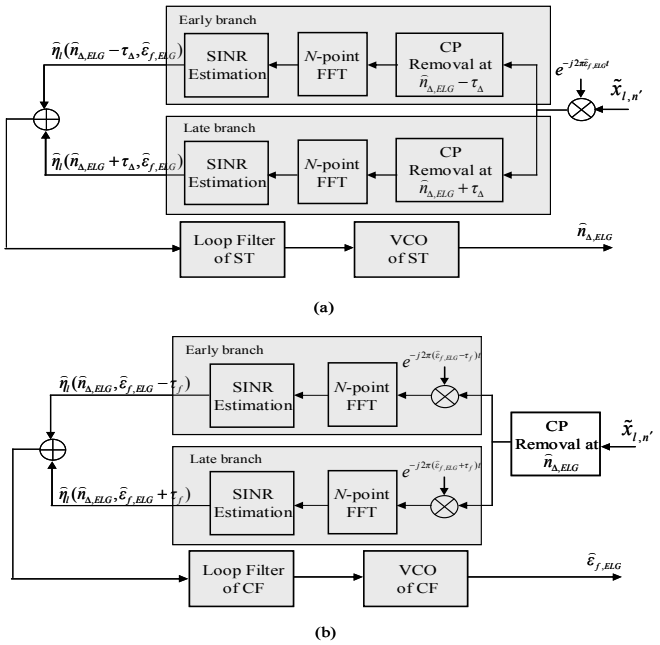

Fig. 3. Architecture of the MSINR ELG synchronization recovery loop: (a) ST synchronizer (b) CF synchronizer. Note that the symbol indices l in $\hat{n}_{\Delta,ELG}(l)$ and $\hat{\varepsilon}_{f,ELG}(l)$ are dropped in this figure for notational simplicity.

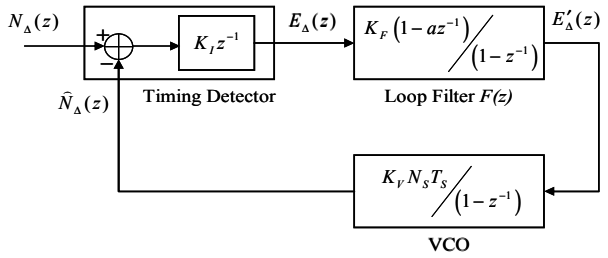

Fig. 4. Approximated discrete-time model of the ELG recovery loop for the ST synchronizer.

where $K_T \triangleq K_F K_I K_V N_S T_S$ is the overall loop gain.

3) MSINR-ELG CF (MSINR-ELG-CF) Recovery Loop: The MSINR CF synchronizer is shown in Fig. 3(b) and is similar to the ST synchronizer except that the signal is assumed to be shifted in frequency early by $\hat{\varepsilon}_{f,ELG}(l)-\tau_f$ and late by $\hat{\varepsilon}_{f,ELG}(l)+\tau_f$, where τ_f is the frequency shift relative to the estimated CFO. The S-curve of the frequency discriminator is given by

$$e_f(l+1) = \hat{\eta}_l(\hat{n}_{\Delta,ELG}(l), \hat{\varepsilon}_{f,ELG}(l)-\tau_f) - \hat{\eta}_l(\hat{n}_{\Delta,ELG}(l), \hat{\varepsilon}_{f,ELG}(l)+\tau_f). \quad (18)$$

Since the CF synchronizer utilizes a similar ELG recovery loop as the ST synchronizer, it is omitted here.

C. ELG Loop Analysis and Design

Before introducing the loop design, it must be emphasized that there is no unique optimum design that can be applied in all conditions to the well-known compromise problem between the loop jitter and acquisition time. By designing for the case of signal-to-noise ratio (SNR) = 20 dB and considering the acquisition range, we set τ_Δ value to 0.25. The intrinsic gain K_I is determined as 32 to best fit the S-curve. The remaining parameters of the ELG loop are configured as: $K_F = 1$, $a = 0.9997$ and $K_V N_S T_S = 2\times10^{-3}$. Finally, K_T can be shown to be 0.064, and the normalized loop bandwidth $BN_S T_S$, where B is the loop bandwidth, can be shown to be 0.02. Therefore, the rise time of the loop is roughly around 50 symbols.

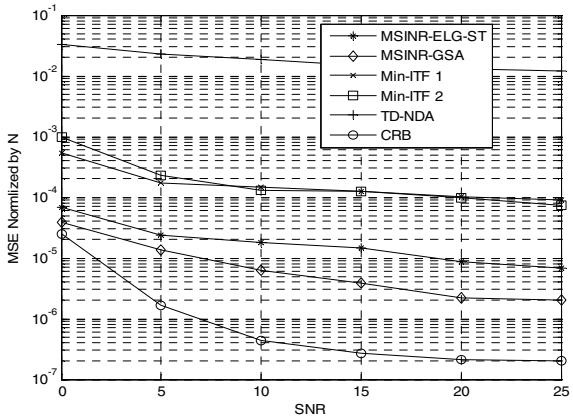

Fig. 5. MSEs of the compared ST synchronizers against the SNR.

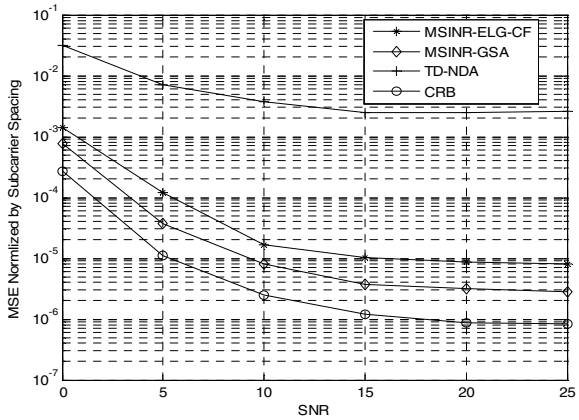

Fig. 6. MSEs of the compared CF synchronizers against the SNR.

D. Computational Complexity

The computational complexity is dominated by four FFTs in Fig. 3. An N-point radix-2 FFT roughly requires $\frac{N}{2}\log_2 N$ complex multiplications. The averaged MSC (11) requires $2N$ complex multiplications and N absolute operations. Finally, the total amount of complexity is $N\left(\frac{1}{2}\log_2 N+2\right)$ complex multiplications and N absolute operations for each (early/late) branch. Two divisions are also required in (11) and (12), which are much less than the FFT operation. The computational complexities of the blind frequency-domain synchronization algorithms of [5] and [6] in terms of complex multiplication are roughly $N\left(\frac{1}{2}\log_2 N+1.5\right)$ and $N\left(\frac{1}{2}\log_2 N+0.75\right)$, respectively. As can be seen, the computational complexity in this work is similar to those in [5] and [6] because the complexity is dominated by the FFT operation, which is the same for all the

This full text paper was peer reviewed at the direction of IEEE Communications Society subject matter experts for publication in the IEEE "GLOBECOM" 2008 proceedings.

compared frequency-domain algorithms.

IV. Performance Analysis

The variance of the tracking loop is approximately proportional to the SINR estimation variance with $1/K_I'^2$ factor, where K_I' is the slope of the S-curve at the ideal synchronization point. Further, if we assume that the ST estimation error is a wide-sense stationary white-noise process, after being filtered by $L(z)$, the mean-squared error (MSE) of the synchronizer can be written as

$$E\left[\left(\hat{n}_{\Delta,ELG}(l)-n_\Delta\right)^2\right] \geq \frac{2}{K_I'^2}\frac{\sigma_{\bar{\eta}}^2}{2\pi j}\oint_C L(z)L(z^{-1})z^{-1}dz \quad (19)$$

where $j=\sqrt{-1}$, and $\sigma_{\bar{\eta}}^2$ is the Cramér-Rao lower bound (CRB) of the SINR estimate in [12, Eq. 67]. The factor 2 in the RHS of (19) comes from the subtraction of the SINR estimates at the early and late synchronization points. The MSE of the CF synchronizer uses the same inequality as (19) except that the characteristic of the S-curve and the closed-loop system equation are replaced with those used for the CF synchronizer.

V. Simulations

We use Monte Carlo simulations to evaluate the performance of the synchronizers, and consider an OFDM system of $N = 256$ subcarriers and a guard interval of $N_G = N/8 = 32$ samples. Only data subcarriers are assumed. The simulated modulation scheme is quadrature phase-shift keying (QPSK). The signal bandwidth is assumed to be 2.5 MHz and the radio frequency is 2.4 GHz. The subcarrier spacing is 8.68 kHz. The OFDM symbol duration is 115.2 μs. The CFO is 10% of subcarrier spacing, i.e., 0.87 kHz, in all simulations. To verify the performance of the proposed technique, the channel is assumed to have N_G paths. The channel taps are randomly generated by independent zero-mean, complex Gaussian variables. In each simulation run, 10,000 OFDM symbols are tested.

1) ST Estimation Performance: For the ST estimation, we compare the proposed technique with the following blind or NDA techniques: (a) Blind minimum-interference ST synchronizer (Min-ITF 1) [6], (b) Blind minimum-interference ST synchronizer (Min-ITF 2) [5], and (c) NDA ML ST synchronizer (TD-NDA) [1]. The MSE of the estimated ST against SNR in multipath fading channels is shown in Fig. 5. In addition to the MSEs of the MSINR-ELG-ST and MSINR-GSA (13), the CRB (19) is also shown. As can be seen, the MSINR synchronizer achieves smaller MSE than the compared synchronizers. In addition, the performance of the MSINR-GSA is better than the MSINR-ELG-ST. However, their performances are not too far apart. Therefore, the complexity can be greatly reduced by the ELG technique while not losing too much performance.

2) CFO Estimation Performance: For the CFO estimation, we compare the proposed technique with the TD-NDA CFO estimation in [1]. The MSE of the estimated CFO (normalized by the subcarrier spacing) against SNR in multipath fading channels is shown in Fig. 6. As can be seen, the ELG technique greatly reduces the complexity of the MSINR-GSA with a close performance to it.

Due to space limitation, the figures that demonstrate the acquisition time are not shown. However, by simulations, it is roughly around 50 symbols as targeted.

VI. Conclusion

In literature, the synchronization problem has been treated by the viewpoint of the estimation theory, for example, the ML approach. In this work, we intuitively deal with this problem by maximizing the SINR. The proposed technique is NDA and independent of the signal structure. It has been shown that the proposed ELG tracking loop is a good compromise between the performance and complexity.

Acknowledgement

This work is supported in part by the grants NSC 95-2219-E-009-004 and MOEA 95-EC-17-A-01-S1-048, Taiwan.

References

[1] J. J. van de Beek, M. Sandell, and P. O. Börjesson, "ML estimation of time and frequency offset in OFDM systems," *IEEE Trans. Signal Process*., vol.45, no.7, pp. 1800-1805, Jul. 1997.

[2] T. M. Schmidl and D. C. Cox, "Robust frequency and timing synchronization for OFDM," *IEEE Trans. Commun.*, vol.45, no.12, pp. 1613-1621, Dec. 1997.

[3] H. Minn, V. K. Bhargava, and K. B. Letaief, "A robust timing and frequency synchronization for OFDM systems," *IEEE Trans. Wireless Commun.*, vol.2, no.4, pp. 822-839, Jul 2003.

[4] M. Speth, S. Fechtel, G. Fock, and H. Meyer, "Optimum receiver design for OFDM-based broadband transmission-part II: a case study," *IEEE Trans. Commun.*, vol.49, no.4, pp. 571-578, Apr. 2001.

[5] Q. Zhu and Z. Liu, "Minimum interference blind time-offset estimation for OFDM systems," *IEEE Trans. Wireless Commun.*, vol.5, no.8, pp. 2136-2142, Aug. 2006.

[6] A. J. AI-Dweik, "A novel non-data-aided symbol timing recovery technique for OFDM systems," *IEEE Trans. Commun.*, vol.54, no.1, pp. 37-40, Jan. 2006.

[7] M. Speth, S. Fechtel, G. Fock, and H. Meyer, "Optimum receiver design for wireless broad-band systems using OFDM-part I," *IEEE Trans. Commun.*, vol.47, no.11, pp. 1668-1677, Nov. 1999.

[8] J. Li and M. Kavehrad, "Effects of time selective multipath fading on OFDM systems for broadband mobile applications," *IEEE Commun. Letters*, vol.3, no.12, pp. 332-334, Dec. 1999.

[9] Y. Mostofi and D. C. Cox, "Mathematical analysis of the impact of timing synchronization errors on the performance of an OFDM system," *IEEE Trans. Commun.*, vol.54, no.2, pp. 226-230, Feb. 2006.

[10] G. C. Carter, C. H. Knapp and A. H. Nuttall, "Estimation of the magnitude-squared coherence function via overlapped fast Fourier transform processing," *IEEE Trans. Audio Electroacoust.*, vol.AU-21, no.4, pp. 337-344, Aug. 1973.

[11] R. W. Lowdermilk and F. J. Harris, "Synthetic instruments extract masked signal parameters," *IEEE Instrum. Meas. Audio Mag.*, vol.8, Issue 3, pp. 40-46, Aug. 2005.

[12] D. R. Pauluzzi and N. C. Beaulieu, "A comparison of SNR estimation techniques for the AWGN channel," *IEEE Trans. Commun.*, vol.48, no.10, pp. 1681-1691, Oct. 2000.